*Current Zoology*, 2024, **70**, 45–58
https://doi.org/10.1093/cz/zoad004
Advance access publication 8 February 2023
**Original Article**

# Collective decision-making and spatial patterns in orientation of an endemic ungulate on the Tibetan Plateau

**Xueting Yan (严雪婷)[a], Xu Wang (王旭)[a], Yumeng Zhao (赵雨梦)[a], Qin Zhu (祝芹)[a], Le Yang (杨乐)[b], Zhongqiu Li (李忠秋) [a,*]**

[a]Lab of Animal Behavior & Conservation, School of Life Sciences, Nanjing University, Nanjing, Jiangsu, 210023, China
[b]Tibet Plateau Institute of Biology, Lhasa, 850000, China.

[*]Address corresponding to Zhongqiu Li. E-mail: lizq@nju.edu.cn
*Handling editor: James F. Hare*

## Abstract

Group living animals form striking aggregation patterns and display synchronization, polarization, and collective intelligence. Though many collective behavioral studies have been conducted on small animals like insects and fish, research on large animals is still rare due to the limited availability of field collective data. We used drones to record videos and analyzed the decision-making and behavioral spatial patterns in orientation of Kiang (Tibetan wild ass, *Equus kiang*). Leadership is unevenly distributed among Kiang, with the minority initiating majority behavior-shift decisions. Decisions of individual to join are driven by imitation between group members, and are largely dependent on the number of members who have already joined. Kiang respond to the behavior and position of neighbors through different strategies. They strongly polarize when moving, therefore adopting a linear alignment. When vigilant, orientation deviation increases as they form a tighter group. They remain scattered while feeding and, in that context, adopt a side-by-side alignment. This study reveals partially-shared decision-making among Kiang, whereby copying neighbors provides the wisdom to thrive in harsh conditions. This study also suggests that animals' spatial patterns in orientation depend largely on their behavioral states in achieving synchronization.

**Key words:** decision-making, imitation, spatial position, Tibetan wild ass

Aggregation is a widespread, ecologically advantageous strategy (Parrish and Edelstein-Keshet 1999; Mann 2018). To maintain group cohesion, group members need to decide when to change their behavior and which behavior to switch to (Beauchamp 2014). Since heterogeneity exists among individuals, the decision of whether and when to join varies extensively (Jolles et al. 2020). A consensus decision in which all members adopt the same behavior is the result of competition and compromise of members (Mann 2018). Synchronization will occur if consensus is reached. How animals make group decisions and what affects the decision-making process have been the focus of considerable research effort (Conradt and Roper 2003; Ramseyer et al. 2009; Torney et al. 2018).

There are two extreme decision-making systems: democracy is when the majority of members decide; autocracy is when one leader decides (Conradt and Roper 2003, 2005). Under most conditions, democratic decisions cost considerably less than autocratic decisions in promoting synchronization, producing less-extreme outcomes (Conradt and Roper 2003). Democracy especially benefits homogeneous groups with members that have similar time budgets, and similar body sizes, because individuals sacrifice less in deviating from optimal time budgets (Conradt and Roper 2003; Jolles et al. 2020). Game theory predicts that democracy will be an evolutionarily stable strategy (ESS) for both homogenous and heterogeneous groups under symmetric consensus cost conditions (changing to an activity too early or too late costs almost the same) (Conradt and Roper 2003, 2007). Partially-shared decision-making is the distribution of leadership falling between two extremes (democracy and autocracy), with some members making the majority of the decisions, while others retain the ability to initiate (Bisazza et al. 2014). Ungulates like cattle show partially-shared decision-making. Homogeneity in age and sex may predispose heifers to favor shared decision-making, yet affinitive bonds resulted in certain individuals taking greater responsibility (Ramseyer et al. 2009).

Making informed decisions requires social information, including the behavior and spatial position of conspecifics (Conradt and Roper 2005; Dahl et al. 2018; Gil et al. 2018). Gathering information imposes time and energy costs (Dall et al. 2005), so the trade-off between information gathering and decision speed requires individuals to choose proper behavior and position themselves according to their needs. Behavior of conspecifics can provide environmental clues: feeding reveals the location of food and a safe environment; vigilance implies an emerging threat; movement suggests impending danger or a preferred destination (Dall et al. 2005). Local position and orientation of conspecifics affect the interaction of group members and global spatial pattern (Couzin et al. 2002). Self-organization theory proposed three simple interaction rules. Individual will move towards distant neighbors to avoid being

Received 11 February 2022; accepted 31 January 2023

separated, align with neighbors to keep group cohesion and move away from over-crowded group members to avoid collision (Couzin et al. 2002; Couzin and Krause 2003). If individuals have a large zone of alignment, the group will exhibit a highly polarized form (Couzin et al. 2002) which benefits the group in attaining food resources at a higher speed (MacGregor et al. 2020). Meanwhile, a disordered group in which individuals face different directions achieves a larger collective visual field and responds more rapidly to food resources (MacGregor et al. 2020) and perhaps predators.

Imitation provides a simple and quick rule to transfer social information in decision-making (Couzin and Krause 2003). Sheep imitate the active or inactive states of conspecifics to remain associated with one another (Gautrais et al. 2007). Caribou imitate the two-dimensional direction of neighbors to form lines (Torney et al. 2018) thereby better conforming to their migration route. Increasing polarization among free-ranging goats *Capra aegagrus hircus* is a product of imitation (Sankey et al. 2021). By imitating adjacent members, individuals benefit from more accurate decision-making and thus enhance individual fitness as well as group stability.

Kiang (the Tibetan wild ass, *Equus kiang*) (Perissodactyla, Equidae) are group-living ungulates that are distributed across high-altitude and remote areas of the Tibetan Plateau, and are one of the largest asses in the world (Schaller 1998; St-Louis and Côté 2009). The species is listed as Least Concern by the International Union for Conservation of Nature (IUCN) but is a Category I species in China. While Kiang became a successful example of animal protection since the population increase in recent years in China, they remain poorly studied (Sharma et al. 2004; Wang et al. 2021). The difficulty of obtaining synchronous and continuous data for each member in the natural setting (Hughey et al. 2018) have rendered its decision-making pattern largely unknown. In recent years, acquiring high-quality and continuous data from the wild has become possible with the development of science and technology. Unmanned aerial vehicles (UAVs, drones) constitute one such technology that has been used increasingly because of its rapid and cost-effective deployment (Hughey et al. 2018). Through remote control, one can easily acquire a comprehensive picture of spatial positions of target species, larger animals especially, from the sky. UAVs provide unprecedentedly flexibility and an effective approach to collect behavioral data (Torney et al. 2018; Inoue et al. 2019), especially for animals inhabiting open areas like the Tibetan Plateau.

Leadership distribution in ungulates varies. Studies of kiang relatives including horses (*Equus caballus* and *Equus ferus przewalskii*) and plains zebra *Equus burchelli* revealed that their decision-making relies on a shared decision-making process with no obvious leader (Bourjade et al. 2009; Andrieu et al. 2016). A study of European bison found that adult females were responsible for most initiation (Ramos et al. 2015). Therefore, it is of value to conduct an in-depth investigation into the decision-making process of Kiang, with behavior states and patterns considered as well.

In this paper, we used drones to collect behavioral data of Kiang. We investigated the leadership distribution, decision joining process, inter-individual relative distance, orientation deviation and position, polarization and alignment of groups to help us better understand the decision-making and spatial pattern of this species. In the present study, we address: (i) Which type of decision-making pattern kiang employ; (ii) How different decisions interact with spatial position and pattern at the individual and group level. We hypothesize that Kiang will employ shared decision-making mainly because the two sexes of this species share similar activity budgets despite female kiang being slightly smaller than males (St-Louis and Côté 2009, 2017). We also predict that behavior would affect both decision and synchronized state because behavior reflects animal needs. Our study uncovers the decision-making pattern of the kiang in the Tibetan Plateau, providing a basic framework for future studies on other ungulate species in the same or adjacent areas.

## Materials and Methods

### Study area and animals

Our study was carried out in July 2020 at Chang Tang Nature Reserve (30°41′–36°41′N, 83°52′–90°26′E) and Siling Co Nature Reserve (30°10′–32°10′N, 87°46′–91°48′E), Tibet, China. The Qinghai-Tibetan Plateau is a unique geographical unit (Jiang et al. 2018). The climate of Chang Tang is harsh and unpredictable because of its high elevation (above 4500 m) and low temperature (annual average temperature is –0.9°C to –3.3°C).

The Tibetan wild ass is included among the National Key Protected Wild Animals Category I in China. The habitat of Kiang includes alpine meadows and alpine steppes. The main predators Kiang face are wolf *Canis lupus* and Tibetan blue bear *Ursus arctos pruinosus*.

## Video processing

### *Video recording.*

We followed previously planned line transects between four counties (Shuanghu, Shenzha, Bange and Nima) every day by car. Each transect was traversed only once over the entire study. Groups encountered on the return trip would not be sampled. Since group activities of Kiang are mostly restricted to certain areas, and no regular migratory patterns have been observed (Schaller 1998), pseudoreplication resulting from recording the same group was reduced. We defined those individuals within 50 m of others as a focal group (Wang et al. 2021).

Before formal recording commenced, we tested a suitable approach route and height to minimize disturbance, while researchers kept at least 300 m away to reduce any observer effect (Li 2011). The drone (Mavic 2 Pro, DJI, China) went up vertically to 120 m above ground level first, and was then flown toward the group. When Kiangs were observed on the monitor, the drone would descend slowly to 100 m above ground. At this height, Kiang showed no signs of being frightened, like sudden acceleration. The distribution of food patches and the environment remained homogeneous, and no predators or obvious disturbances were observed during each recording session, so it was reasonable to infer that collective decisions were intrinsically motivated.

In formal recording, we launched the drone when we saw a group of Kiang, following the protocol described above. Recording started after the drone was above Kiang for at least 1 min and no signs of Kiang escaping were observed. Videos of Kiang were recorded from 09:00 to 12:00 and 16:00 to 18:30 (GMT+8). The camera's shooting angle was 60° to ensure behavior changes could be recorded. The drone was not flown in rain, snow or strong winds. Thus, all videos were recorded in sunny or cloudy weather. We followed each group for 10-20 min depending on drone battery life.

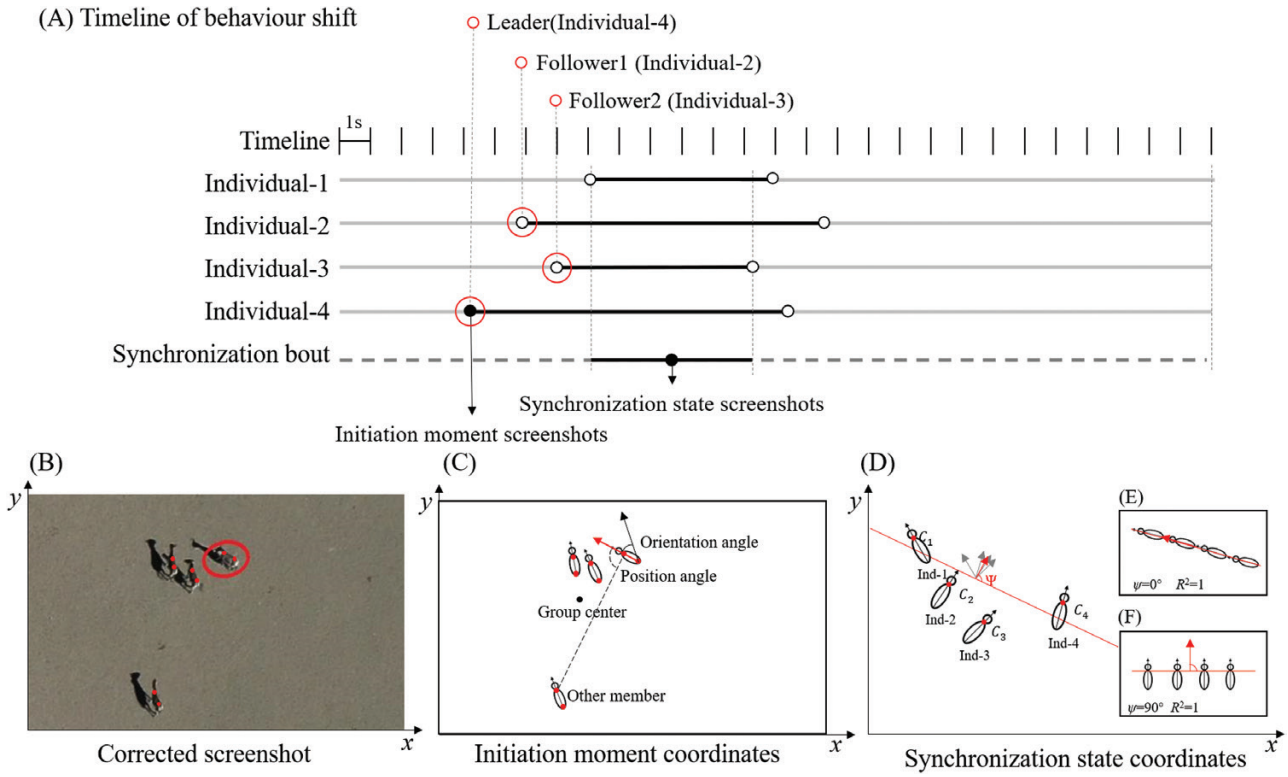


**Figure 1. Timeline of behavior shift and spatial data extraction for *Equus kiang*.** (A) synchronization bout means the time when all members perform the same behavior. Red open dots represent the leader (with black closed dot) and the first two followers (with black open dots). Black lines represent that the individual was doing the target behavior (can be feeding, moving or vigilance). (B) Corrected screenshot, where red circle highlights the leader. Red dots are the shoulder and rump of Kiangs. (C) Spatial coordinates (red closed dots), orientation (black arrow), orientation angle and position angle of members. Angle between dashed line and leader orientation is the position angle of target individual. (D) $C_1$ (grey arrow) represents vector of body position of individual 1, $C_2$, $C_3$, $C_4$ have (grey arrows) similar meaning. Red line means linear fitting line, $k$ is the slope of red line. (E)&(F): ψ stands for the angle between group direction (red arrow) and the alignment fit line (red line), range from 0°-90°. (E): an example of extreme linear formation in line of the group with ψ equals to 0, $R^2$ of fit line and *Op* equals to 1. (F): an example of extreme side-by-side alignment of the group with ψ equals to 90, $R^2$ of fit line and *Op* equals to 1.

### *Reviewing behavior timeline of each member.*

For each group, we first numbered every member at the beginning of the video, then manually tracked each Kiang and scored its behavior. Each member eventually had its identity and a timeline of behavior shifts (Figure 1A). The same process was adopted for 25 h of videos from 94 groups. The sex and age of individuals were indistinguishable due to their similar body size and appearance. The drone's shooting angle and the distance between the observers and Kiang prevented us from recognizing their genitals. Foals were included in the study because no obvious differences were observed between the behavior of foals and adults. Behaviors were classified into feeding, moving, vigilance, and other types. We defined feeding as an individual's head down below the shoulder apparently seeking food or water or chewing food; moving as walking, trotting, and running with head up; vigilance as individuals standing still and scanning their surroundings (Jiang 2000; Li 2016) (behavior definition in Fig A1).

### *Taking screenshots.*

We took screenshots using PotPlayer (Kakao Corp., South Korea) at the moment of decision initiation and upon the achievement of synchronization to document the spatial pattern associated with those stages of collective decision making (Figure 1).

### *Correcting distorted drone image (screenshots).*

The camera's shooting angle caused image distortion. To calculate relative inter-individual distance more accurately, we applied a perspective transformation to correct images. Image correction was performed by MATLAB (MathWorks Inc., U.S.A.) based on OpenCV (see details in Supplementary material_Image Correction). After the correction, the actual length and width of the image (Figure S1.1) had about a 3% bias.

### *Obtaining coordinates.*

We used the open-source image-processing platform Image J (NIH, U.S.A.) to get coordinates of individuals to calculate relative distance, position and orientations. The polarization (*Op*, Order parameter) and alignment (goodness of fit: $R^2$; alignment angle: $\psi$) for groups were further calculated. The orientation of an individual was represented by the vector $C_i$(unit vector of $(x_i,y_i)$). It stands for the rump-to-shoulder direction of individual $i$in the two-dimensional picture. Point coordinates of individual $i$'s shoulder are $(SX_i,SY_i)$. Coordinates of the group centre are

$$\text{group center} = \left(\frac{\sum_{i=1}^{n} SX_i}{n}, \frac{\sum_{i=1}^{n} SY_i}{n}\right) \quad (1)$$

At the group level, group direction is a vector:

$$C_g = \left( x_g = \frac{\sum_{i=1}^{n} x_i}{\sqrt{(\sum_{i=1}^{n} x_i)^2 + (\sum_{i=1}^{n} y_i)^2}}, y_g = \frac{\sum_{i=1}^{n} y_i}{\sqrt{(\sum_{i=1}^{n} x_i)^2 + (\sum_{i=1}^{n} y_i)^2}} \right) \quad (2)$$

where $n$ is the group size.

*Order Parameter* ($Op$), ranging from 0 to 1, is the parameter to evaluate how strong group members faced in the same direction. The stronger the order, the bigger $Op$ (Vicsek et al. 1995; Couzin et al. 2002; MacGregor et al. 2020).

$$Op = \frac{\sqrt{(\sum_{i=1}^{n} x_i)^2 + (\sum_{i=1}^{n} y_i)^2}}{n} \quad (3)$$

The alignment fit line was computed from coordinates of members' shoulders to see if individuals were aligned linearly or not, with $R^2$ evaluating the goodness of fit and $k$ evaluating its slope. Only when $R^2$ and $Op$ are both close to 1, does the calculation of alignment angle make sense: $\psi$ measures the angle between group direction and the direction of the alignment fit line ($k$), ranging from 0° to 90°. $\psi$ equals 0° means all individuals line up in the orientation direction; $\psi$ equals 90° means all individuals are aligned side by side (Figure 1E, F).

$$\psi = \arccos\left( \frac{((\sum_{i=1}^{n} x_i) + k \cdot (\sum_{i=1}^{n} y_i))}{\sqrt{k^2 + 1}} \right) \times \frac{180}{\pi} \quad (4)$$

## Decision making

### *Definitions of decision making.*

When an individual changes its behavior, we considered this shift as an attempt. Only when an attempt is responded to by at least two other members, was it called a decision. The individual that initiates the decision is defined as the leader, and those who respond are called followers. A decision requires followers to shift to the same behavior (target behavior) as the leader before the leader made its next shift. Since an individual changing its behavior may not intend to recruit others, we do not define an attempt without any followers as a failure or a decision. We initially manually recorded every behavior-shift in the videos and followed the timeline to identify the leader and any followers. The moment when a leader shifted its behavior is the decision initiation moment. We defined "habitual leader" as an individual that behaved as leader more frequently than it behaved as follower. Conversely, "habitual follower" was an individual that behaved more often as follower. Neutral represented individuals who showed no inclination to lead or follow, and non-joiner were ones who never lead nor follow. Leading preference focused only on individual performance and was represented by leading times divided by the sum of an individual's leading times and following times, helping us to identify if particular members were more likely to lead. Decision time is the time between the behavior-shift of the leader and the response of the last follower. Decision latency is the time between the behavior-shift of a follower and the previous follower.

### *Calculation of Leadership and Gini Coefficient.*

If a group with $n$ members had $D$ decisions, the leadership score of each Kiang ($i$) was calculated as follows: total number of times individual $i$ behaved as leader ($d_i$) divided by the sum of decisions ($D$) in the group ($L_i = d_i/D$). Standard leadership score ($L_i$ -$1/n$) provides a comparison between individuals in the same group.

We used the Gini coefficient (G), which is commonly used to evaluate income inequality, to quantify the degree of inequality of leadership distribution among Kiangs. G was originally applied to evaluate wealth distribution in countries. However, G is also seen in biology and sociology to measure the inequality of certain values. It was used to quantify the inequality of flight activity among honeybees (Tenczar et al. 2014) and inequality of cooperative behavior among groups (Rotics and Clutton-Brock 2021). While there are many ways to calculate G, all methods are mathematically equal. The adjusted Gini coefficient ($G_a$, based on absolute difference) is calculated as "one half of the relative mean difference between every pair of data in an infinite population". We chose the equation which corrects small group size bias (Bowles and Carlin 2020; Banerjee et al. 2021). $G_a$ ranges from 0 (perfectly equal) to 1(completely unequal).

$$G = \frac{\sum_i^n \sum_j^n |d_i - d_j|}{2\mu(d)\, n\, (n-1)} \quad (5)$$

Where, $i$ and $j$ are the individuals in the group; $d_i$ is the number of times individual $i$ behaved as leader and $d_j$ is the number of times individual $j$ behaved as leader; $|d_i - d_j|$ is the absolute difference of the leadership score between individual $i$ and $j$; $\mu(d)$ is the average leading times of the group members; and $n$ is the group size. For $\mu(d) = D/n$ and $Li = d_i/D$, the final equation is adjusted as below:

$$G_a = \frac{\sum_i^n \sum_j^n |L_i - L_j|}{2\,(n-1)} \quad (6)$$

Where, $G_a$ stands for the adjusted Gini coefficient of leadership distribution; $L_i$ and $L_j$ are leadership scores of individual $i$ and $j$.

### *Joining process.*

We studied average latencies for followers who joined group behavior-shift decisions (i.e. the latency of a follower $j$ is the time between the behavior-shift of follower $j$ and the previous follower $j$-$1$) by performing survival analysis and curve estimation. A linear distribution of the survival curve reveals that the probability of a Kiang joining the decision is dependent on time, while a power or exponential distribution means that this probability is not dependent on time but rather on the number of individuals that have already joined the movement (Sueur et al. 2009; Ramos et al. 2015). In addition, we used curve estimation to test the relation between the distribution of average latencies and the joining rank of followers. If this distribution shows a parabolic curve, the joining process can be inferred to be a mimetic phenomenon (Ramos et al. 2015).

### *Spatial patterns in orientation of decision initiation moment.*

Among all decisions included in the previous analysis, we selected three types of decision (decisions that shift to feeding, moving and vigilance) for each group based on two requirements with different priority: 1) involved as many followers as possible; 2) led by a habitual leader if one exists. For the second requirement, we wanted to ensure that decisions were led by habitual leaders so that the preference of position is clear. If no decisions meet the requirements, we selected randomly. After the selection, we went back to the original video to take screenshots at the moments when the leader starts the shift (decision initiation moment) and

highlighted the leader. We took 151 screenshots from 54 groups to stand for decision initiation moments (50 feeding; 54 moving; 48 vigilance) (Figure 1A, C, Table A4). 4 or 6 groups lacked decisions we needed, so fewer than 54 screenshots were obtained for certain behavior types. Image correction and coordinate were obtained as described in the *Video processing* session.

We calculated relative distance, relative position and orientation angles for all members relative to leaders by setting the leader's shoulder as the origin, and leader orientation as vector (0,1) in a polar coordinate system (Figure 1.c). Relative distance was calculated as distance divided by the body length of the leader. We also calculated the relative distance of members to the group center. To evaluate remoteness of the leader in the group, we divided the relative distance of the leader with group center by the maximum relative distance of all group members to group center. If remoteness of the leader was close to 1, the leader was close to the group edge. We also calculated polarization ($Op$) and alignment (goodness of fit: $R^2$ and alignment angle: $\psi$) for each screenshot representing the initiation moment as described above in the *Definitions of decision-making* section.

## Synchronization

### *Spatial patterns in orientation of synchronization state.*

We took screenshots at the middle point of each synchronization bout (when all members act the same behavior for at least 3 seconds) (Figure 1 A, D) to represent the synchronized state. Synchronization state may occur even when no decision as defined above happens, and thus we included all synchronized states as long as they satisfied our definition. We obtained 1216 screenshots (693 feeding; 437 moving; 86 vigilance) out of 94 groups to investigate the space-use difference between behaviors. Spatial information was extracted from corrected screenshots (Figure 1.d). At the group level, we calculated Order parameter ($Op$) and alignment (goodness of fit: $R^2$ and alignment angle: $\psi$) for each screenshot that represents the synchronized state as described above in the *Obtaining coordinates* section. For each pair of individuals, the relative distance was calculated based on the distance of the individual's shoulder ($SX_i$, $SY_i$) and average body length (shoulder to rump) of all group members. If the relative distance of individual $i$ and individual $j$ equals 2, it means that the distance between their shoulders is 2 times the average body length of current group members. The angle of their orientations was calculated by

$$\text{orientation deviation} = \arccos\left(x_i x_j + y_i y_j\right) \quad (7)$$

## Data Analysis

Statistical analyses except GLMM were carried out with SPSS 25.0 (IBM Corp., U.S.A.) whereas the graphs were made using Origin 2019 (OriginLab Corp., U.S.A.). GLMMs were modelled by R 4.2.2 (R Core Team, 2022) using packages *lme4* (Bates et al. 2015) and *glmmTMB* (Brooks et al. 2017). Probability distributions of all original data of response variables were tested by R package *fitdistrplus* (Delignette-Muller and Dutang 2015) (see details in supplementary material). The level of statistical significance was set at $P = 0.05$. All data were reported as mean ± *SE*.

### *Data analysis of leadership, Gini coefficient of leadership distribution.*

Because the count of decisions is an integer, we selected 54 groups with each group having at least $n$ ($n$ = group size) decisions to guarantee each member has at least one time to lead if the decision is equally shared (1661 decisions in total). For each individual, we determined the correlation between leadership score and leading propensity using a Spearman correlation test. We also tested whether the leadership score differed between habitual leaders and habitual followers using a Wilcoxon paired-sample test. We calculated $G_a$ (adjusted Gini coefficient based on absolute difference) and tested its normality using a Shapiro–Wilk test. Then we analyzed correlations between $G_a$, group size, number of habitual leaders and times of decision using Spearman correlation tests.

### *Data analysis of difference between decisions that shift to different behaviour.*

Among decisions that have been selected in analyzing the Gini coefficient (1661 decisions from 54 groups), we focused on the decisions whose previous behavior and target behavior are feeding, moving or vigilance (1522 decisions) (Table A4.). We compared decision time and latency of different previous behavior and target behavior using Friedman tests.

### *Data analysis of spatial pattern in orientation difference that shift to different behavior.*

We applied GLMM to evaluate the effect of behavior (feeding, moving and vigilance) on spatial choice of non-leaders. All tests were two tailed. Before GLMM, *position angle* was transformed to 0-180° to eliminate periodicity implicit in circular data (Cremers and Klugkist 2018). Beta distribution and the logit link function were used for response variables *position angle* and *orientation deviation* after they have been transformed to 0-1. A Gamma distribution and the inverse link function were used for the response variable *relative distance* (Sun and Ronnegard 2011). The *previous behavior* (categorical with 3 levels), *target behavior* (categorical with 3 levels) and *group size* were entered as fixed factors. The *group identity* was entered as a random factor to incorporate the dependency among data derived from the same group. We compared leader distance to center, goodness of fit ($R^2$), order parameter ($Op$) and alignment angle ($\psi$) of the decision initiation moments that shift to different target behavior using Friedman tests.

### *Data analysis of synchronization state.*

We applied GLMM to evaluate the effect of behavior (feeding, moving and vigilance) on spatial choice of group members when they are in a synchronized state. Beta distribution and the logit link function were used for response variables $Op$, $R^2$ and $\psi$ of each synchronized state. Gamma distribution and the inverse link function were used for response variables *orientation angle* and *relative distance*, of all paired-individuals as they were continuous positive and non-normally distributed after we fit their distribution in R. *Synchronized behavior* (categorical with 3 levels), *group size* and the interaction between *group size* and *synchronized behavior* were entered as fixed factors. The *group identity* was entered as a random factor to incorporate the dependency among data from the same group.

## Results

A total of 25 h of video was recorded from 94 groups. Group size ranged from 3 to 32. (9.57 ± 0.59 on average). We selected 54 groups with at least *n* (group size) decisions to investigate the Gini coefficient, joining process and pattern in orientation and position. We took 1,216 snapshots that reflected the synchronization state for different behaviors (693 for feeding; 437 for moving; 86 for vigilance) to investigate spatial pattern in orientation at the individual and group level. More sampling information is in Appendix Table A4.

### Decision making

#### *Leadership distribution and Gini Coefficient.*

Gini coefficient ($G_a$) of leadership distribution among 54 Kiang groups followed a normal distribution (Shapiro–Wilk Statistics = 0.958, $P$ = 0.057) with a mean of 0.422 ($SE$ = 0.017), and range from 0.216 to 0.750 (Figure 2A). Leadership inequality became stronger with an increase in the number of group members and habitual leaders (Table A1). $G_a$ was positively correlated with group size (Spearman's $\rho$ = 0.356, $P$ = 0.008) and the number of habitual leaders (Spearman's $\rho$ = 0.413, $P$ = 0.002), while no significant correlation between $G_a$ and the number of decisions within group was evident ($P$ = 0.109).

In Kiang, individuals play different roles in leading behavior-shifting decisions. In each group, only 0-3 individuals are habitual leaders (about 13% of group members). Among individuals, the standard leadership score of habitual leaders (0.104 ± 0.012) is significantly higher than that of habitual followers (-0.019 ± 0.003) (Wilcoxon paired-sample test, $P$ < 0.001). Leadership scores of habitual leaders were clustered above evenly shared leadership (Figure 2B), confirming that if a group member was inclined to lead rather than to follow, it was more likely to lead than others. In addition, higher leadership score often comes with longer feeding time (Table A2).

#### *Survival analysis of joining process.*

Survival analysis and curve estimation showed that latency of joining a decision follows an exponential ($R^2$ = 0.878, $F_{1,701}$ = 5026.567, $P$ < 0.001, $y = 0.6153e^{-0.1121x}$) or power ($R^2$ = 0.873, $F_{1,701}$ = 4797.269, $P$ < 0.001, $y = 1.2043x^{-1.0432}$, $R^2_{exponential} > R^2_{power} > R^2_{linear}$) distribution rather than a linear distribution ($R^2$ = 0.433, $F_{1,701}$ = 534.831, $P$ < 0.001, $y = -0.0195x + 0.5624$), indicating that the joining process depended on the number of individual who have already joined (Figure 3A). The distribution of mean latency according to the joining rank of followers followed a parabolic curve ($R^2$ = 0.217, $F_{2,23}$ = 3.194, $P$ = 0.06, $y = 0.0265x^2 - 0.8149x + 9.3699$), confirming a mimetic mechanism underlying joining a decision (Figure 3B).

There are differences between decisions that shift to different target behaviors. Survival analysis revealed that joining a feeding decision was significantly slower than joining decisions to shift to moving according to the curve fit (Log Rank Mantel-Cox, *Chi-square* = 84.808, $P$ < 0.001) or to vigilance (Log Rank Mantel-Cox, *Chi-square* = 46.265, P < 0.001) (Table 1 & Fig A2). This finding agrees with that from the comparison of decision times (Friedman-test, *Chi-square* = 14.489, $P$ = 0.001, *df* = 2) and latencies (Friedman-test, *Chi-square* = 33.396, $P$ < 0.001, *df* = 2): when Kiang shift to feeding, decision time (27.8 ± 1.6 s) and latency (7.4 ± 0.4 s) were significantly longer than decisions that shift to moving (decision time 16.1 ± 0.9 s, latency 4.4 ± 0.3 s) or to vigilance (decision time 18.2 ± 2.0 s, latency 4.6 ± 0.3 s) (Figure 4). Decision times (Friedman-test, *Chi-square* = 0.659, $P$ = 0.719, *df* = 2) and latencies (Friedman-test, *Chi-square* = 0.123, $P$ = 0.940, *df* = 2) did not differ, however, among the possible behavior types Kiang shifted from.

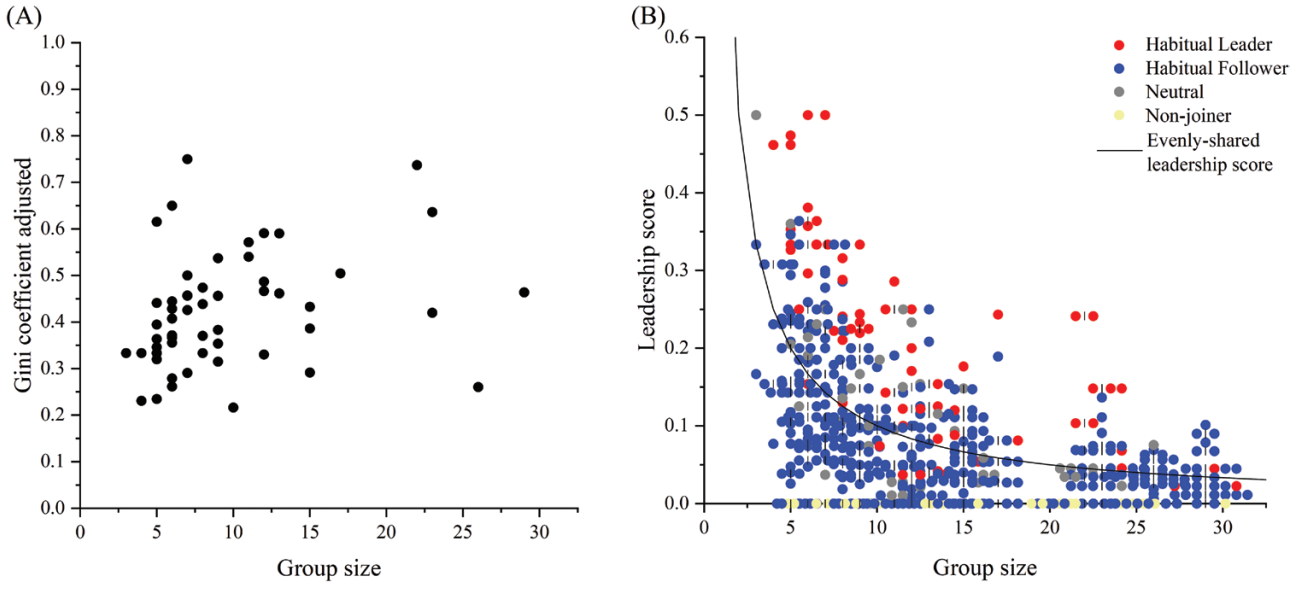


**Figure 2. Gini coefficient of leadership distribution and leadership score of individuals.** (A) Adjusted Gini coefficient of each group according to group size. (B) Leadership score of individuals according to group size. Black line represents leadership score when leadership was evenly-shared among group members (1/n). Red dots represent habitual leader, blue dots represent habitual follower, grey dots represent neutral individual who are not inclined to lead or follow. Yellow dots represent those who did not follow nor lead. Bar between two dots is to offset overlapped dots.

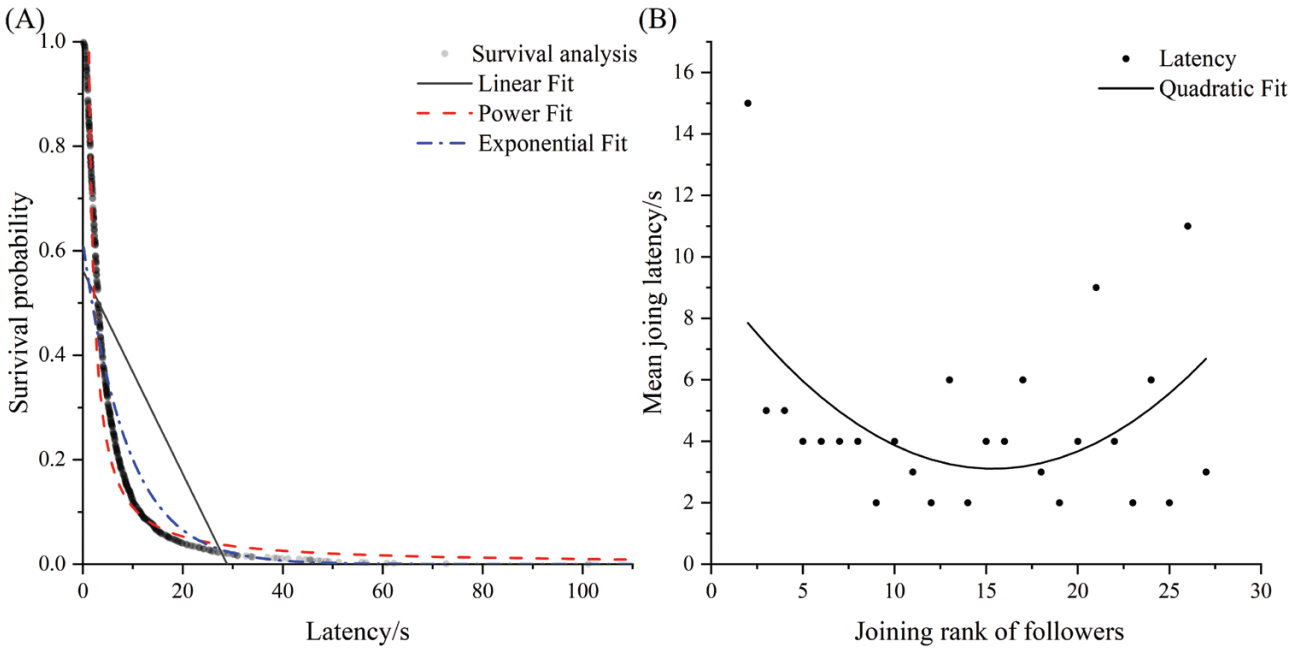


**Figure 3. Distribution of decision latencies.** (A) Survival analysis and estimated distribution of joining latencies. The semi-transparent black dots represent cumulative survival probability, the grey continuous line stands for linear distribution, the red dashed line stands for power distribution and the blue dash-dot line represents exponential distribution. (B) Mean joining latency according to the rank of followers. Dots represent mean latency for each rank, while the best-fit line is a parabolic function.

**Table 1.** Curve estimation of joining latencies of survival probability for different target behavior.

| Target behavior | Function | $R^2$ | $F$ | $P$ | Equation |
|---|---|---|---|---|---|
| Feeding | Linear | 0.564 | 475.442 | <0.001 | y=-0.0211x + 0.6184 |
| | Power | 0.856 | 2190.165 | <0.001 | $y=1.6755\ x^{-1.0014}$ |
| | **Exponential** | **0.956** | **7883.995** | **<0.001** | **$y=0.7632\ e^{-0.1044x}$** |
| Moving | Linear | 0.406 | 249.658 | <0.001 | y=-0.0282x + 0.5987 |
| | Power | 0.848 | 2036.739 | <0.001 | $y=0.9439x^{-1.0403}$ |
| | **Exponential** | **0.819** | **1655.827** | **<0.001** | **$y=0.6479e^{-0.1514x}$** |
| Vigilance | Linear | 0.554 | 265.002 | <0.001 | y=-0.0398x + 0.6637 |
| | Power | 0.870 | 1428.452 | <0.001 | $y=1.1050\ x^{-1.0742}$ |
| | **Exponential** | **0.933** | **2970.483** | **<0.001** | **$y=0.8153e^{-0.1879x}$** |

Function with largest $R^2$ values were in bold.

## Spatial patterns in orientation

### *Spatial patterns in orientation in decision initiation moment.*

At the group level, no apparent spatial pattern was evident in decision initiation moments because alignment angle ($\psi$), order parameter ($Op$) and goodness of fit ($R^2$) did not differ among decisions that shifted to different behavior types (Friedman-test, $\psi$: *Chi-square* = 0.304, $P$ = 0.859, $df$ = 2; $Op$: *Chi-square* = 2.652, $P$ = 0.266, $df$ = 2; $R^2$: *Chi-square* = 1.696, $P$ = 0.428, $df$ = 2) (Figure 5A). Leaders were closer to the group edge rather than the group center with a relative distance to the group center of 0.623 ± 0.024 (Figure 5B). Since goodness of fit ($R^2$) was small (0.528 ± 0.027) (Figure 5.b), individuals did not tend to align linearly, and thus calculating alignment angle does not make any sense (Figure 5C).

Though individuals were spread around leaders, their mean position was behind the orientation of the leader (mean position angle = 180.22 ± 3.36°) with a mean orientation angle of 41.33 ± 1.22° (Figure 6). On one hand, GLMM showed that group size had no significant effect on position and orientation choice of non-leaders. On the other hand, previous and target behavior significantly affected position choice (Table 2). Non-leaders positioned themselves more to the back of the leader when they shift from moving, and position angle increased more so with a shift to moving than with a shift to feeding (Table 2).

### *Spatial patterns in orientation of synchronization state.*

At the group level, GLMM revealed different spatial distribution strategies when Kiang synchronized behavior differed. $Op$, goodness of fit ($R^2$) and $\psi$ were significantly affected by synchronized behavior (Table 3). At the group level, when all Kiang were feeding, $\psi$ was distributed between 60-90° (62.11 ± 0.75°) with average $Op$ of 0.76 ± 0.01° (Figure 7), indicating that Kiang line up in the

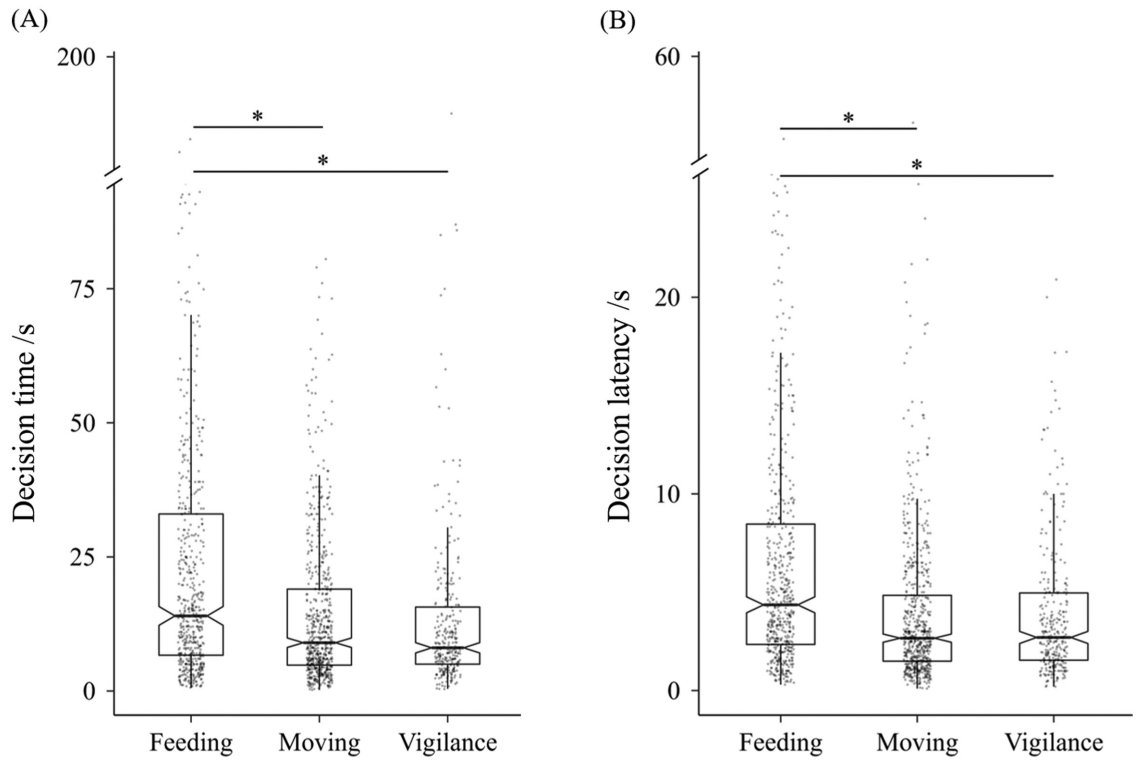


**Figure 4. Boxplot of decision latency and decision time.** Note: The notches in the boxes show 95% confidence intervals for the medians. * represents that the decision time (A) and latency (B) were significantly different ($P < 0.05$) in Friedman test when Kiang shift to different target behavior.

horizontal direction in a more disorderly state. They are inclined to stand side by side, leaving the abdomen sheltered by others. When all individuals moved, they strongly followed the same direction with *Op* being 0.96 ± 0.01° and tended to arrange themselves linearly as $\psi$ ranged between 0-30° (33.19 ± 1.10°) (Figure 7). For collective vigilance, no specific spatial distribution appeared.

At the individual level, inter-individual orientations deviation and relative distance were significantly affected by group size and synchronized behavior (Table 3). Individual orientation deviated significantly more when Kiang were vigilant and showed minimal angular deviation when they were moving (Table 3). Also, individuals were significantly closer to each other when vigilant and maintained greater inter-individual distances relative to others when they were foraging and moving (Table 3). They copied neighbors' directions when they were collectively moving.

## Discussion

This is the first empirical study to investigate the collective decision-making of the ungulate *Equus kiang*. We analyzed data from 54 groups of Kiang and found that decisions to shift between behavioral states are predicated upon partially-shared decision-making. Furthermore, decisions to shift to feeding are made more slowly than decisions to move or become vigilant. GLMMs revealed different spatial patterns in the synchronized state. When feeding, they scatter. When moving, they form lines. When vigilant, they get closer to each other yet face different directions.

Kiang practiced partially-shared decision-making via imitation. As we hypothesized, most group members in *Equus kiang* had a chance to initiate a decision (Figure 2B). Gini coefficient analysis suggests leadership is unequally distributed (Figure 2), Whereby a small number of individuals are responsible for the majority of initiations (Figure 2B). In extremely heterogeneous groups, the minority benefit more than the rest, which may result in unequal leadership distribution (Conradt and Roper 2003). Though Kiang's sexual dimorphism is subtle (St-Louis and Côté 2009), heterogeneity may play an important role in prompting leadership inequality. Heterogeneity in sex, age, experience, personality and energy level affect the decision-system and how individuals react to their environment (Ramos et al. 2015; Jolles et al. 2020). In European bison (*Bison bonasus*), female adult and male sub-adult initiators have a higher likelihood of successful initiations and therefore stronger leadership (Ramos et al. 2015). Kiang groups typically have several adults with their young (nursery group) or without foals, or exist as bachelor groups (St-Louis and Côté 2017; Wang et al. 2021). In nursery groups, females may require more energy and invest more time on feeding, thus creating heterogeneity in the group (St-Louis and Côté 2012). In bachelor groups, social class of male Kiang affects their activity budget (Kannan and Parsons 2017), which may affect their consensus cost in reaching a collective decision. We found habitual leaders have a higher chance of playing the leading role in the group. A study of cows, *Bos taurus*, reported that dominant cows in agonistic interaction have a stronger influence in leading movement (Sarova et al. 2010). Therefore, it is likely that individual traits and personal inclination affect leadership. Leaders positioned themselves on the periphery of their group (Figure 5B) and had a higher probability of being at the front of their group (Figure 6A). This result coincides with spatial sorting before movement departure where leaders tend to take the front position in horse groups (Briard et al. 2021). Future

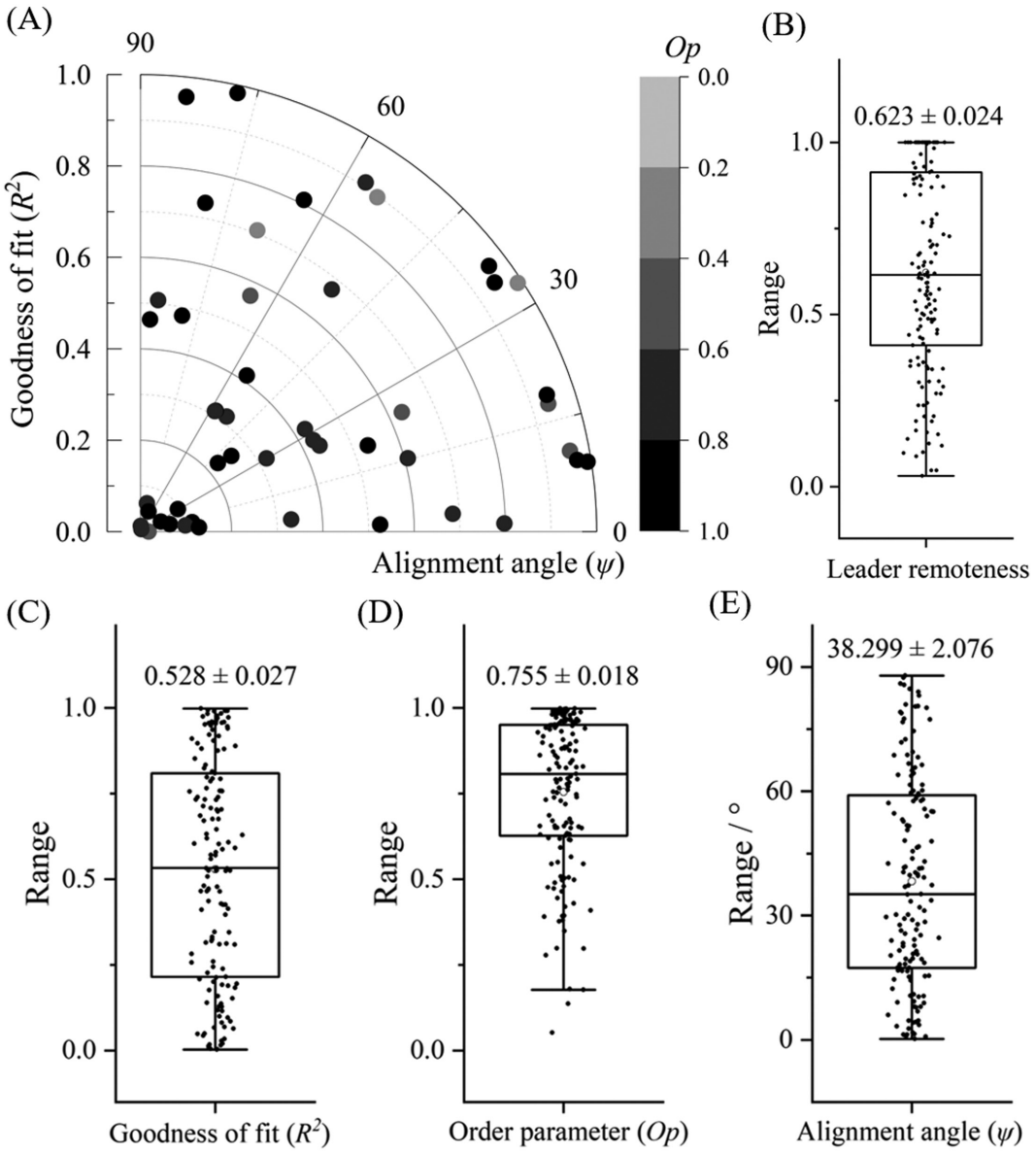


**Figure 5. Spatial pattern in decision initiation moment.** (A) Alignment of Kiang group. (B) Boxplot of leader distance to group center. (C) Boxplot of goodness of fit ($R^2$) of Kiang alignment. (d) Boxplot of order parameter ($Op$) of Kiang orientation. (E) Boxplot of Alignment angle (ψ). Mean ± standard error is shown above the box. The box plots show the median and 25th and 75th percentiles; the whiskers indicate the values within 1.5 times the interquartile range.

research on individual traits, positioning and social structure of Kiang are required to better understand the role individuals play in decision-making.

The asymmetric cost in behavior-shifting decisions may also explain leadership inequality. Shifting to foraging no matter how early or late costs no more than lost food intake in that short period of time. But, shifting to vigilance or moving too late may cost an individual its life in a high predation risk condition, while shifting too early would cost relatively little. Since overall predation risk is unlikely to threaten Kiang (St-Louis and Côté 2009), asymmetries among the three behaviors may be low. Game theory predicts that in a strong asymmetric case, autocracy may be favored because following the action of a sole leader would reduce evaluation costs (Conradt and Roper 2007). In the weak asymmetric case of Kiang, partially-shared decision-making may represent a compromise.

In terms of the mechanism underlying the joining process, whether Kiang join in on a decision depends on how many individuals have already joined, which exemplifies quorum-based decision-making, since survival analysis and curve estimation revealed that their latency to join followed an exponential or power function rather a linear function (Figure 3). This result supported the hypothesis of shared decision-making whereby the majority would eventually join and make a collective behavior-shift. Imitation mechanisms are evident through the process of copying behavior-shift in joining latency – the more members that joined, the shorter the latency was (Figure 3). The mimetic mechanism underlying choices of Kiang is corroborated by our spatial polarization results. The order parameter increases from the initiation moment through to the synchronized state (Figure 5&7). Such alignment in posture could result in a stronger tendency to imitate and more frequent synchronization bouts in ungulates (McDougall and Ruckstuhl 2018). As described

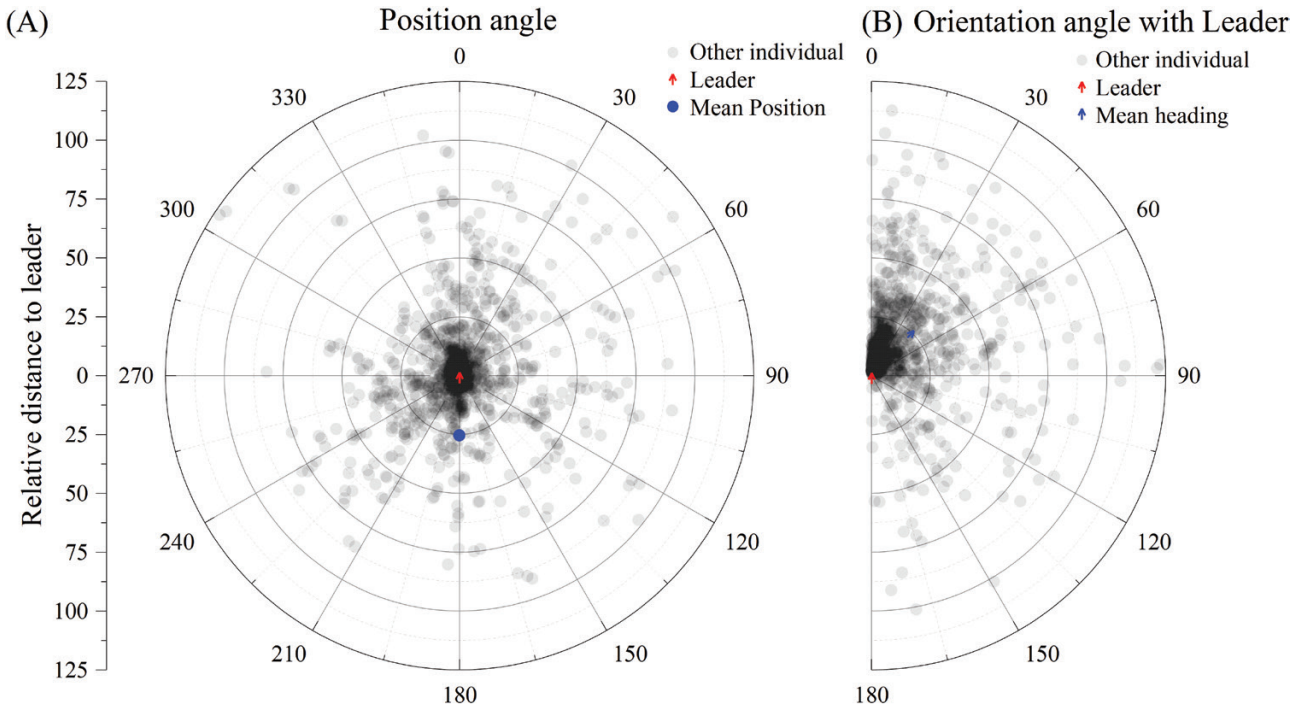


**Figure 6. Position and orientation angle compared with leader.** (A) Relative position of non-leaders. (B) Orientation angle with leader. Red arrow represents leader's body orientation. Grey dots represent the relative position of other individuals. Blue dot is the mean position angle of other individuals. Blue arrow is the mean orientation of other individuals. Relative distance is calculated as distance of shoulder coordinates of individual and leader divided by body length of leader.

**Table 2.** Results of GLMMs evaluating the effect of behaviour and group size on the spatial choice (position angle, orientation deviation and relative distance) of non-leaders.

| | *Estimate* | *Std.error* | *t-value* | *P-value* |
|---|---|---|---|---|
| ***Position angle*** *(Beta, logit link)* | | | | |
| Intercept | **−0.639** | **0.213** | **−3.004** | **0.003** |
| *Group Size* | −0.001 | 0.014 | −0.069 | 0.945 |
| *Previous Behavior-Moving* | **0.311** | **0.135** | **2.304** | **0.021** |
| *Previous Behavior-Vigilance* | 0.063 | 0.131 | 0.483 | 0.629 |
| *Target Behavior-Moving* | **0.593** | **0.142** | **4.190** | **<0.001** |
| *Target Behavior-Vigilance* | **0.478** | **0.097** | **4.933** | **<0.001** |
| ***Orientation deviation*** *(Beta, logit link)* | | | | |
| Intercept | **−1.367** | **0.186** | **−7.348** | **<0.001** |
| *Group Size* | 0.010 | 0.012 | 0.807 | 0.420 |
| *Previous Behavior-Moving* | −0.085 | 0.117 | −0.726 | 0.468 |
| *Previous Behavior-Vigilance* | 0.163 | 0.114 | 1.424 | 0.154 |
| *Target Behavior-Moving* | −0.075 | 0.123 | −0.610 | 0.542 |
| *Target Behavior-Vigilance* | 0.112 | 0.084 | 1.336 | 0.182 |
| ***Relative distance*** *(Gamma, Inverse link)* | | | | |
| *Intercept* | **0.031** | **0.005** | **6.132** | **<0.001** |
| *Group Size* | **<0.001** | **0.000** | **−2.403** | **0.016** |
| *Previous Behavior-Moving* | **0.010** | **0.004** | **2.410** | **0.016** |
| *Previous Behavior-Vigilance* | **0.011** | **0.005** | **2.295** | **0.022** |
| *Target Behavior-Moving* | **0.012** | **0.005** | **2.758** | **0.006** |
| *Target Behavior-Vigilance* | **0.015** | **0.004** | **4.003** | **<0.001** |

*P* values below 0.05 are in bold.

in goats, the consensus direction results from imitation rather than voting (Sankey et al. 2021). Spatial patterns in orientation vary according to behaviors. Many studies have focused only on movement decisions (Amornbunchornvej and Berger-Wolf 2019), yet behavior affects how animals decide. Contrary to our expectation, at the decision initiation moment, neither the

**Table 3.** Results of GLMMs evaluating the effect of behaviour, group size on the group spatial pattern (*Op*, $R^2$, ψ) and inter-individual orientation deviation and relative distance.

| | Estimate | Std.Error | t value | P value |
|---|---|---|---|---|
| *Op* (Beta, logit link) | | | | |
| Intercept | **1.930** | **0.147** | **13.167** | **<0.001** |
| Group size | **−0.101** | **0.020** | **−5.086** | **<0.001** |
| Synchronized behaviour-Moving | **1.027** | **0.175** | **5.863** | **<0.001** |
| Synchronized behaviour-Vigilance | −0.492 | 0.314 | −1.566 | 0.117 |
| Group size*Moving | 0.043 | 0.023 | 1.818 | 0.069 |
| Group size*Vigilance | 0.095 | 0.055 | 1.736 | 0.083 |
| $R^2$ (Beta, logit link) | | | | |
| Intercept | 0.195 | 0.185 | 1.051 | 0.293 |
| Group size | −0.025 | 0.026 | −0.941 | 0.347 |
| Synchronized behaviour-Moving | 0.418 | 0.225 | 1.853 | 0.064 |
| Synchronized behaviour-Vigilance | **0.809** | **0.407** | **1.985** | **0.047** |
| Group size*Moving | −0.014 | 0.031 | −0.470 | 0.638 |
| Group size*Vigilance | −0.098 | 0.072 | −1.358 | 0.175 |
| ψ (Beta, logit link) | | | | |
| Intercept | **0.649** | **0.143** | **4.542** | **<0.001** |
| Group size | 0.022 | 0.021 | 1.064 | 0.288 |
| Synchronized behaviour-Moving | **−1.374** | **0.176** | **−7.821** | **<0.001** |
| Synchronized behaviour-Vigilance | **0.675** | **0.316** | **2.138** | **0.033** |
| Group size*Moving | 0.021 | 0.024 | 0.859 | 0.390 |
| Group size*Vigilance | **−0.164** | **0.055** | **−2.982** | **0.003** |
| **Orientation deviation** (Gamma, Inverse link) | | | | |
| Intercept | **0.016** | **<0.001** | **39.638** | **<0.001** |
| Group size | **<0.001** | **<0.001** | **8.180** | **<0.001** |
| Synchronized behaviour-Moving | **0.044** | **0.001** | **36.543** | **<0.001** |
| Synchronized behaviour-Vigilance | −0.001 | 0.003 | −0.504 | 0.614 |
| Group size*Moving | **−0.001** | **<0.001** | **−12.176** | **<0.001** |
| Group size*Vigilance | 0.001 | <0.001 | 2.355 | 0.018 |
| **Distance** (Gamma, Inverse link) | | | | |
| Intercept | **1.014** | **0.018** | **55.987** | **<0.001** |
| Group size | **−0.012** | **0.002** | **−6.552** | **<0.001** |
| Synchronized behaviour-Moving | **0.347** | **0.029** | **11.885** | **<0.001** |
| Synchronized behaviour-Vigilance | **0.567** | **0.162** | **3.496** | **<0.001** |
| Group size*Moving | **−0.012** | **0.003** | **−4.693** | **<0.001** |
| Group size*Vigilance | −0.014 | 0.025 | −0.561 | 0.575 |

*P* values below 0.05 are in bold.

previous nor target behavior had significant effects on spatial pattern at the group level (Figure 5A). Yet in the synchronized state, spatial pattern varied according to behavior (Figure 7 & Table 3). Kiangs in the active state (moving) were more polarized than in the static state (feeding and vigilance) (Table 3), indicating that the level of activity influences space-use (Michelena et al. 2008). At the individual level, both previous behavior and target behavior had significant effects on positions and distance (Table 2). At the latter stage (synchronized state), inter-individual distance and orientation deviation were also significantly affected by behavior (Table 3).

The Qinghai-Tibetan Plateau presents unique environmental conditions that shape animal behavior (St-Louis and Côté 2009). High altitude and low oxygen levels force Kiang to save energy. Kiang also need to consider both predation risk and foraging benefits when choosing their position in the group (Inoue et al. 2019). Meanwhile, behavior and position affect visual field and thus social information (Strandburg-Peshkin et al. 2013; MacGregor et al. 2020). With their head down, as is typically the case while feeding, Kiang lose sight of their surroundings; even with their head up, blind spots in the rearward direction exist (McGreevy 2004). Individuals need to adjust their position and orientation to cooperate with neighbours and to cover a larger collective visual field. When feeding, orientation deviation was larger and the relative distance was greater than for any other behavior. This scattering tendency from the moment of initiation to the synchronized state may result from intragroup competition on foraging pastures. In the synchronized feeding state, Kiang exhibited side-by-side alignment which may benefit individuals by covering themselves with their neighbors' bodies (Beauchamp 2014). Moving consumes more energy than other activities

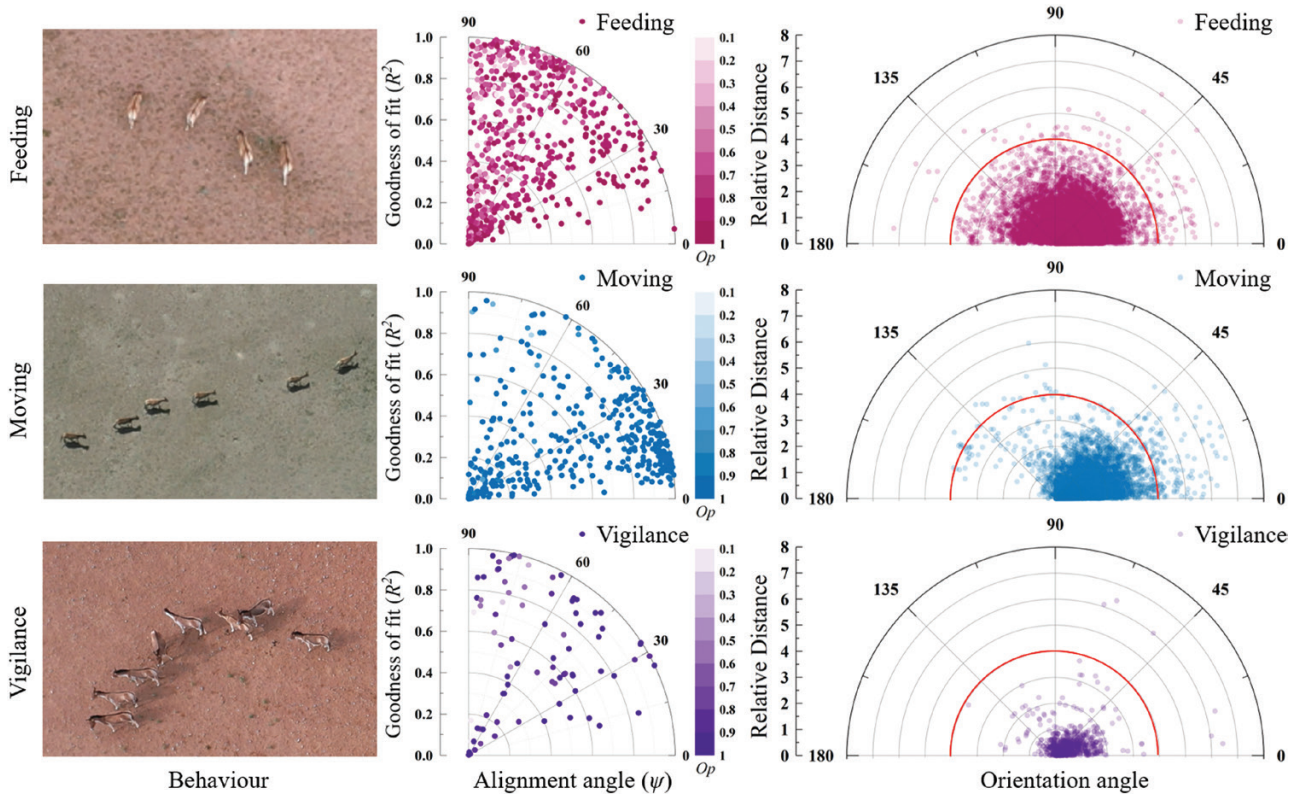


**Figure 7. Spatial distribution differs with behavior in synchronization state.** First column: Behavior snapshot of *E. kiang*. From the top is synchronized feeding, moving, and vigilance. The second column is the Alignment of three synchronized behaviors. The third column is the Relative distance and orientation deviation of the paired individuals in the synchronized state. *Op*: Order parameter, the closer to 1.0, the stronger the order. Goodness of fit was computed by the shoulder position of all individuals. the angle was calculated by the difference of composite vector and *k* of fit line.

in ungulates (Brosh et al. 2010). The linear alignment is common in movement decisions among ungulates (Torney et al. 2018; Sankey et al. 2021). Kiang also formed a linear alignment when moving (Fig 6). Linear alignment may especially save followers energy when running (Spence et al. 2012). A study of aerodynamic drafting in horses revealed that individuals in a drafting position perform better (Spence et al. 2012).

Vigilance showed a denser space-use strategy both at the moment of initiation and in the synchronized state (Table 2&3). When facing potential external threat, individuals may seek cover within the group which creates a tight pattern in space (Beauchamp 2014; Fryxell and Berdahl 2018). The greatest orientation deviation from leaders appeared in the context of vigilance (Table 2), which may benefit individuals by providing more social information owing to an increased collective visual field (Strandburg-Peshkin et al. 2013). In achieving this collective vigilance, Kiang depart from the direct copying rule that promotes synchrony evident in other group behavioral states.

The use of drones holds exceptional promise for documenting behavior relative to telemetry collars and GPS devices since the latter two require animal capture and equipment attachment. However, limited battery life constrained the sampling time. Inequal leadership distribution was more likely to happen in short periods. Sampling groups multiple times over a longer period of time may diminish potential bias. More work needs to be done to further investigate how information regarding sex, age, energy level and experience of individuals, and the social hierarchy within groups affect leadership distribution.

Our study provides specific patterns of Kiang positioning and orientation when engaged in different behaviors, which will facilitate the recognition of critical Kiang foraging grounds and movement corridors fromsatellite photographs so that the Chinese government can identify regions requiring protection. Traditional surveys have been constrained by the accessibility of roads (Zhang et al. 2022), but using satellite photographs requires less survey effort and covers more area. Moreover, whereas most studies focused only on movement decisions, our study reveals that behavior also plays an important role in decision-making. This study also provides an index with which to compare leadership distribution across groups or species.

## Author contributions

XT Yan and ZQ Li conceived and designed the study. ZQ Li and L Yang provided funding support and fieldwork direction. XT Yan, X Wang conducted fieldwork and collected data with the assistance of YM Zhao. XT Yan, X Wang and Q Zhu processed, analysed and visualized the data. XT Yan wrote the first manuscript draft and ZQ Li, X Wang, YM Zhao, Q Zhu and L Yang reviewed and edited manuscript drafts. All authors read the draft and contributed to the discussion and completion of the final manuscript.

## Acknowledgment

We are grateful to HZ Si and JQ Hu for their contribution on programming. Additional thanks are due to ZW Zhang, Andi, F Yu, XX Wang for their field help; C Yu, CJ Fu and XX Wang for critical comments; Sana Ullah for language proofreading. We express our deepest gratitude to reviewers and editors

who provided insightful comments and vastly improved the quality of the final manuscript.

## Funding

The work was supported by Tibet Major Science and Technology Project (XZ201901-GA-06), National Natural Science Foundation of China (32101237&41871294) and National key research and development program (2022YFC3202104).

## Conflict of interest

All authors declared no conflict of interests.

## Supplementary Material

Supplementary material can be found at https://academic.oup.com/cz.

## References

Amornbunchornvej C, Berger-Wolf YT, 2019. Mining and modeling complex leadership followership dynamics of movement data. *Soc Net Anal Min* **9**:9–58.

Andrieu J, Henry S, Hausberger M, Thierry B, 2016. Informed horses are influential in group movements, but they may avoid leading. *Anim Cogn* **19**:451–458.

Banerjee I, Warnier M, Brazier FMT, Helbing D, 2021. Introducing participatory fairness in emergency communication can support self-organization for survival. *Sci Rep* **11**:1–9.

Bates D, Maechler M, Bolker B, Walker S, 2015. Fitting linear mixed-effects models using lme4. *J Stat Softw* **67**:1–48.

Beauchamp G, 2014. *The Selfish Herd*. London: Academic Press.

Bisazza A, Butterworth B, Piffer L, Bahrami B, Miletto Petrazzini ME et al., 2014. Collective enhancement of numerical acuity by meritocratic leadership in fish. *Sci Rep* **4**:4560.

Bourjade M, Thierry B, Maumy M, Petit O, 2009. Decision-making in Przewalski horses *Equus ferus przewalskii* is driven by the ecological contexts of collective movements. *Ethology* **115**:321–330.

Bowles S, Carlin W, 2020. Inequality as experienced difference: A reformulation of the Gini coefficient. *Econ Lett* **186**:108789.

Briard L, Deneubourg J-L, Petit O, 2021. Group behaviours and individual spatial sorting before departure predict the dynamics of collective movements in horses. *Anim Behav* **174**:115–125.

Brooks ME, Kristensen K, van Benthem KJ, Magnusson A, Berg CW et al., 2017. glmmTMB balances speed and flexibility among packages for zero-inflated generalized linear mixed modeling. *The R Journal* **9**:378–400.

Brosh A, Henkin Z, Ungar ED, Dolev A, Shabtay A et al., 2010. Energy cost of activities and locomotion of grazing cows: A repeated study in larger plots. *J Anim Sci* **88**:315–323.

Conradt L, Roper TJ, 2003. Group decision-making in animals. *Nature* **421**:155–158.

Conradt L, Roper TJ, 2005. Consensus decision making in animals. *Trends Ecol Evol* **20**:449–456.

Conradt L, Roper TJ, 2007. Democracy in animals: The evolution of shared group decisions. *Proc Royal Soc B* **274**:2317–2326.

Couzin ID, Krause J, 2003. Self-organization and collective behavior in vertebrates. *Adv Study Behav* **32**:1–75.

Couzin ID, Krause J, James R, Ruxton GD, Franks NR, 2002. Collective memory and spatial sorting in animal groups. *J Theor Biol* **218**:1–11.

Cremers J, Klugkist I, 2018. One direction? A tutorial for circular data analysis using R with examples in cognitive psychology. *Front Psychol* **9**:2040.

Dahl CD, Wyss C, Zuberbuhler K, Bachmann I, 2018. Social information in equine movement gestalts. *Anim Cogn* **21**:583–594.

Dall SR, Giraldeau LA, Olsson O, McNamara JM, Stephens DW, 2005. Information and its use by animals in evolutionary ecology. *Trends Ecol Evol* **20**:187–193.

Delignette-Muller ML, Dutang C, 2015. fitdistrplus: An R package for fitting distributions. *J Stat Softw* **64**:1–34.

Fryxell JM, Berdahl AM, 2018. Fitness trade-offs of group formation and movement by Thomson's gazelles in the Serengeti ecosystem. *Phil Trans R. Soc B*. **373**:20170013.

Gautrais J, Michelena P, Sibbald A, Bon R, Deneubourg J-L, 2007. Allelomimetic synchronization in Merino sheep. *Anim Behav* **74**:1443–1454.

Gil MA, Hein AM, Spiegel O, Baskett ML, Sih A, 2018. Social information links individual behavior to population and community dynamics. *Trends Ecol Evol* **33**:535–548.

Hughey LF, Hein AM, Strandburg-Peshkin A, Jensen FH, 2018. Challenges and solutions for studying collective animal behaviour in the wild. *Phil Trans R Soc B* **373**:20170005.

Inoue S, Yamamoto S, Ringhofer M, Mendonca RS, Pereira C et al., 2019. Spatial positioning of individuals in a group of feral horses: A case study using drone technology. *Mamm Rev* **64**:249–259.

Jiang ZG, 2000. PAE coding system for the behaviors of the Père David' s deer. *Acta Theriol Sin* **20**:1–12.

Jiang Z, Li L, Hu Y, Hu H, Li C et al., 2018. Diversity and endemism of ungulates on the qinghai-tibetan plateau: Evolution and conservation. *Biodiv Sci* **26**:158–170.

Jolles JW, King AJ, Killen SS, 2020. The role of individual heterogeneity in collective animal behaviour. *Trends Ecol Evol* **35**:278–291.

Kannan PM, Parsons MH, 2017. Social class and group size as predictors of behavior in male *Equus kiang*. *Anim Beh Cogn* **4**:442–454.

Li Z-Q, 2016. Datasets of vigilance behavior for three rare ungulates. *Biodiv Sci* **24**:1335–1340.

Li Z, 2011. Suitable distance to observe red-crowned cranes: A note on the observer effect. *Chin Birds* **2**:147–151.

MacGregor HEA, Herbert-Read JE, Ioannou CC, 2020. Information can explain the dynamics of group order in animal collective behaviour. *Nat Commun* **11**:2737.

Mann RP, 2018. Collective decision making by rational individuals. *Proc Natl Acad Sci* **115**:e10387–E10396.

McDougall PL, Ruckstuhl KE, 2018. Doing what your neighbour does: Neighbour proximity, familiarity and postural alignment increase behavioural mimicry. *Anim Behav* **135**:177–185.

McGreevy P, 2004. *Equine Behavior, a Guide for Veterinarians and Equine Scientists*. Edinburgh: W. B. Saunders.

Michelena P, Gautrais J, Gerard J-F, Bon R, Deneubourg J-L, 2008. Social cohesion in groups of sheep: Effect of activity level, sex composition and group size. *Appl Anim Behav Sci* **112**:81–93.

Rotics S, Clutton-Brock T, 2021. Group size increases inequality in cooperative behaviour. *Proc Biol Sci* **288**:20202104.

Parrish JK, Edelstein-Keshet L, 1999. Complexity, pattern, and evolutionary trade-offs in animal aggregation. *Science* **284**:99–101.

Ramos A, Petit O, Longour P, Pasquaretta C, Sueur C, 2015. Collective decision making during group movements in European bison, *Bison bonasus*. *Anim Behav* **109**:149–160.

Ramseyer A, Thierry B, Boissy A, Dumont B, 2009. Decision-making processes in group departures of cattle. *Ethology* **115**:948–957.

R Core Team, 2022. *R: A Language and Environment for Statistical Computing*. Vienna, Austria: R Foundation for Statistical Computing. https://www.R-project.org/.

Sankey DWE, O'Bryan LR, Garnier S, Cowlishaw G, Hopkins P et al., 2021. Consensus of travel direction is achieved by simple copying, not voting, in free-ranging goats. *R Soc Open Sci* **8**:11.

Sarova R, Spinka M, Panama JLA, Simecek P, 2010. Graded leadership by dominant animals in a herd of female beef cattle on pasture. *Anim Behav* **79**:1037–1045.

Schaller GB, 1998. *Wildlife of the Tibetan Steppe*. Chicago: Chicago University Press.

Sharma BD, Clevers J, Graaf RD, Chapagain NR, 2004. Mapping *Equus kiang* (Tibetan wild ass) habitat in Surkhang, Upper Mustang, Nepal. *Mt Res Dev* **24**:149–156.

Spence AJ, Thurman AS, Maher MJ, Wilson AM, 2012. Speed, pacing strategy and aerodynamic drafting in thoroughbred horse racing. *Biol Lett* **8**:678–681.

St-Louis A, Côté SD, 2012. Foraging behaviour at multiple temporal scales in a wild alpine equid. *Oecologia* **169**:167–176.

St-Louis A, Côté SD, 2009. *Equus kiang* (Perissodactyla: Equidae). *Mamm Species* **835**:1–11.

St-Louis A, Côté SD, 2017. Activity budgets and behavioural synchrony in a wild equid living in a fission-fusion social system. *Behaviour* **154**:357–376.

Strandburg-Peshkin A, Twomey CR, Bode NW, Kao AB, Katz Y et al., 2013. Visual sensory networks and effective information transfer in animal groups. *Curr Biol* **23**:R709–R711.

Sueur C, Petit O, Deneubourg JL, 2009. Selective mimetism at departure in collective movements of *Macaca tonkeana*: An experimental and theoretical approach. *Anim Behav* **78**:1087–1095.

Sun L, Ronnegard L, 2011. *Comparison of Different Estimation Methods for Linear Mixed Models and Generalized Linear Mixed Models*. Sweden: Dalarna University.

Tenczar P, Lutz CC, Rao VD, Goldenfeld N, Robinson GE, 2014. Automated monitoring reveals extreme interindividual variation and plasticity in honeybee foraging activity levels. *Anim Behav* **95**:41–48.

Torney CJ, Lamont M, Debell L, Angohiatok RJ, Leclerc LM et al., 2018. Inferring the rules of social interaction in migrating caribou. *Phil Trans R Soc B* **373**:20170385.

Vicsek T, Czirok A, Ben-Jacob E, Cohen II, Shochet O, 1995. Novel type of phase transition in a system of self-driven particles. *Phy Rev Lett* **75**:1226–1229.

Wang XX, Yang L, Zhao YM, Yu C, Li ZQ et al., 2021. The group size effect and synchronization of vigilance in the Tibetan wild ass. *Curr Zool* **67**:11–16.

Zhang L, Li Q, Kou X, Ouyang Z, 2022. Distributions of two native ungulates at the third pole are highly sensitive to global warming. *Glob Ecol Conserv* **39**:e02292.